A simple and versatile machine for creep testing at low loads (6–300 N) and on miniaturized specimens: Application to a Mg-base alloy

N. T. B. N. Koundinya, Nandha Kumar E, Niraj Chawake, Rajesh Korla, and Ravi Sankar Kottada

Citation: Review of Scientific Instruments **89**, 105102 (2018); doi: 10.1063/1.5040841
View online: https://doi.org/10.1063/1.5040841
View Table of Contents: http://aip.scitation.org/toc/rsi/89/10
Published by the American Institute of Physics

A simple and versatile machine for creep testing at low loads (6–300 N) and on miniaturized specimens: Application to a Mg-base alloy

N. T. B. N. Koundinya,[1] Nandha Kumar E,[1] Niraj Chawake,[1,a)] Rajesh Korla,[2,b)] and Ravi Sankar Kottada[1,c)]
[1]*Department of Metallurgical and Materials Engineering, Indian Institute of Technology Madras, Chennai 600 036, India*
[2]*Department of Materials Engineering, Indian Institute of Science, Bengaluru 560 012, India*

(Received 21 May 2018; accepted 10 September 2018; published online 1 October 2018)

High temperature creep testing at a very low load range (<10 N) on miniaturized specimens has always been a challenge due to inherent design limitation (such as significant preload) of the conventional creep testing machines. In the present study, the challenge was overcome by developing a simple and versatile horizontal creep testing machine to conduct creep tests in the loading range of ~6–300 N in tension and in compression. The competence of the in-house-built horizontal creep machine was validated by conducting creep testing on dog-bone shaped sheet specimens of cast Mg-1Sn-1Ca (TX11) Mg-base alloy over a lower stress range of 1.6–5.9 MPa (equivalent load range of 6.4–18.1 N) at 450 °C and in the high stress range of 20–80 MPa (equivalent load range of 76–310 N) at 175 °C. *Published by AIP Publishing.* https://doi.org/10.1063/1.5040841

I. INTRODUCTION

Creep is time-dependent plastic deformation of materials at constant load or stress at temperatures above ~0.4 T_m, where T_m is the absolute melting point.[1,2] To develop high temperature materials for any given application requires a better understanding of the deformation mechanisms of the materials at elevated temperatures, and such an understanding is possible using extensive creep studies. In the last few decades, Mg and Al alloys have found potential applications in automobile and space applications. The scope of the applications of these alloys can be enhanced further by improving their creep properties especially at very low stresses for designing lightweight automobile components at temperatures >0.5 T_m for an extended duration of more than 500 h.[3] Majority of the automobile components are produced through casting, and they experience variable cooling rates depending upon the complexity of the geometry during solidification, resulting in a gradient microstructure across the component.[4–6] In addition, processing routes such as selective laser melting, additive manufacturing, compound casting, and fusion state joining processes can also result in gradient microstructures.[7] The presence of the inhomogeneous and heterogeneous microstructures across the component can lead to multiple creep mechanisms operating in the localised regions. It is important to note that creep testing of bulk samples with heterogeneous microstructure using conventional (bulkier load train and lever arm) creep machines without using modern strain mapping techniques viz. digital image correlation (DIC) may lead to spurious evaluation of the creep properties. This necessitates the need for high temperature creep testing of miniaturized specimens from the intended regions of the actual component or prototypes. These creep tests on miniaturized specimens can shed light on the understanding of creep mechanisms locally operating in these regions. Thus, there is a need to address this issue, and consequently, a creep testing methodology which uses miniaturized specimens over a wide range of stress and temperature is essential.

Evaluation of room temperature mechanical properties using miniaturized specimens under a quasi-static condition has been widely explored, and the results are consistent with the tests performed using the specimens of the American Society for Testing and Materials (ASTM) standard dimensions.[8,9] However, not much attention has been devoted in the literature towards the usage of miniaturized specimens for creep testing at elevated temperatures. This lacuna provides the motivation to establish a methodology for creep testing of miniaturized specimens. The following text in the present section summarizes the literature on existing creep testing methods, their feasibility, and efficacy toward creep testing using miniaturized specimens.

Since the very first report by Andrade in 1910 on constant stress creep testing setup using the hyperbolic weight, there has been a progressive evolution in the creep testing machines and methods.[10] Table I presents a brief review on the progress of the work reported in connection with constant load/stress creep testing.[10–23] It is interesting to note that the most common characteristic feature among all the creep machines is the vertical loading configuration. In this configuration, the specimen is held between two crossheads positioned one above the other. Among the two crossheads, one is fixed (top/bottom) and the other is movable and connected to the load pan. Further, the design of the creep test

a)Present address: Erich Schmid Institute of Materials Science, Jahnstrasse 12, 8700 Leoben, Austria.
b)Present address: Department of Materials Science and Metallurgical Engineering, Indian Institute of Technology Hyderabad, Kandi, Sangareddy 502285, India.
c)Author to whom correspondence should be addressed: ravi.sankar@iitm.ac.in and raviskottada@gmail.com. Telephone: +91 44 2257 4779.

TABLE I. Chronological development of the creep testing methodology. (RT refers to Room temperature).

Authors (year)	Material tested	Test temperature (°C)	Technical advancement	Limitations
Andrade (1910)[10]	Pb–Sn wire	15–162	Constant load and stress creep testing machine—constant stress is achieved using hyperbolic weights sinking into a liquid with known density	Limited only to thin wires in tension
Andrade *et al.* (1932)[11]	Cu, Sn, Al	−180 to 100	Wide stress range during testing was achieved using predesigned cam and lever arm	Only thin wires of specified length can be tested in tension
Nadai *et al.* (1936)[12]	Cu	RT	Constant stress creep testing machine controlled using an electric circuit	Universalization (creep and stress relaxation) of the setup is cumbersome
Hopkin (1950)[13]	Pb	RT	High accuracy constant stress creep machine using the cam design	Limited to fixed specimen dimension and loading mode due to pre-designed cam
Kennedy *et al.* (1956)[14]	...	...	Constant stress and load using an electromechanical control system for strains >5%	Limited to a specific range of loads for constant stress maintenance
Boettner *et al.* (1956)[15]	...	...	Constant stress using the cam design to a higher accuracy using drop/pickup of weights	Limited to large specimens and restricts the universalization of loading
Dudderar (1969)[16]	Pb–Sn	RT	Constant stress up to 2000% using the cam design and balancing weights	Sensitive to specimen dimensions and restricts the universalization of loading
Solomon (1969)[17]	Fe-3% Si, Al	500–800, 250–300	Constant stress and load using the servo controlled hydraulic system	Achieving the low loads is hard due to the hydraulic system
Coghlan (1972)[18]	Al	384–450	Constant stress using the pre-designed cam profile during compression	Limited to large specimens and restricts the universalization of loading for low loads
Yavari *et al.* (1982)[19]	Al-5% Mg	550	Constant stress and very low loads using modified cam geometry and counterweight	Limited to large specimens and restricts the universalization of loading for low loads
Grishaber *et al.* (1997)[20]	Al 2009/15/SiCw	350	Constant stress using the servo-controller using a computer	Constrained to standard specimens in a higher load range
Kolbe *et al.* (1999)[21]	Nickel based superalloy	1100	Constant load creep testing on miniature tensile specimens with direct loads	Restricted to high strength alloys
Völkl *et al.* (2004)[22]	Pt-10% Rh	1500	Ultra-high temperature creep testing machine with constant stress but aimed for shorter duration of testing	For shorter duration and standard specimens
Luan *et al.* (2017)[23]	Nimonic-75	850–1000	Constant load creep testing with miniature tensile specimens for lower loads	Limited to a low load range and challenging in universalization of loading

frames can be broadly classified into two categories: (i) lever arm based where it is possible to apply high loads with the help of high mechanical advantage and (ii) constant stress creep test frame using proper cam design. However, with a cam design, for each sample size, separate cam needs to be designed. In addition to the above-mentioned creep testing jigs, electromechanical machines are also developed where the load/stress can be applied by pulling or pushing the specimen using a closed-loop controlled electric motor.[20]

While dealing with the creep testing of low melting point (<950 K) materials such as Mg-base and Al-base alloys, one of the parameters that needs attention is the preload on the specimen during creep testing. It is the load on the specimen before application of the actual test load and also it is the minimum load that can be neither avoided nor ignored. Usually, in a lever-arm type or motor-driven conventional tensile creep machines, the pull-rods and specimen fixtures add considerable preload on the specimen which is more than the allowable preload, especially for specimens with a lower area of cross section and testing at lower stresses. Higher preload can result in the modification of the initial microstructure before application of the actual load. In fact, the ASTM standards (ASTM E139-11) stipulates that the preload during creep testing should be <10% (considering the material yield stress) of the actual load for reliable results during creep testing.[24] This is usually achieved with the usage of the specimens with larger cross-sectional areas. To access lower loads on the standard specimens, Coghlan,[18] and Yavari and Langdon[19] independently built vertical type constant stress compression and tensile creep testing machines, respectively. However, these are not of the universal (tension and compression) type and have limitations with the usage of miniaturized specimens. Besides, accessing the high-stress range, application to miniaturized specimens is also not possible due to the inherent limitations in the design of these machines. Hence, it is evident that a universal creep machine design in terms of accessing lower loads of <15 N while enabling a wide stress range of creep testing, minimization of the excessive preload, and universal (tension and compression) testing methodology for miniaturized specimens has not been addressed in the open literature.

Recently, a miniature specimen geometry for creep testing was reported by Kolbe *et al.* to perform creep experiments on directionally solidified (DS) single crystal superalloys and aluminum composites using non-ASTM standard creep specimens.[21,25,26] However, the stress corresponding to the preload was estimated to be ~2.5 MPa (15 N), which is significantly higher for the light metals such as Al/Mg and their alloys. Apart from this study, a few other research groups also substantiated the applicability of miniaturized specimens for creep testing and reported a decent agreement between miniaturized creep specimen testing and conventional creep testing of bulk specimens.[27–37] Nevertheless, it is important to note that the total applied load is much higher than 15 N in most of these studies. Also, more importantly, the preload applied before the creep testing was not reported in majority of these studies.

Based on the comprehensive discussion presented above, the primary issues with most of the conventional creep testing machines are as follows: (a) unavoidable preload, which can significantly alter the test results, especially in low strength and low melting point alloys such as Mg-base and Al-base alloys, and (b) lack of feasibility to do universal (tension and compression) creep testing of miniaturized specimens over a large stress range starting from loads <10 N. Further, it would be ideal if a creep machine is versatile so that additional modules such as digital image correlation (DIC) can be integrated easily as attachments.

Evaluation of the capability of a designed horizontal creep testing machine over a wide range of loads is important. In view of this, creep testing of an Mg-base alloy (since it is a candidate material for automobile power train components) is essential. It is noteworthy to mention that most of the creep studies on the rare-earth-free cast magnesium alloys were carried out in the temperature range of 150–200 °C (applied stress of 20–120 MPa), while magnesium composites were tested above 200 °C (applied stress of 7–125 MPa), and various creep mechanisms were reported to be operating during creep.[5,38,39] Creep tests on solid solution Mg-0.8Al have shown that viscous glide (stress exponent of 3) is the rate controlling mechanism at stresses lower than 20 MPa.[40] However, a stress exponent of 1.5 was reported for the die cast AC53 magnesium alloy at 175 °C in the stress range of 42–70 MPa, and grain boundary sliding (GBS) was suggested as the operating mechanism.[41] Thus, there is an ambiguity on the rate controlling mechanism in the lower stress range. This scenario has motivated us to validate the efficacy of the in-house-built horizontal creep frame by studying the creep behavior of the as-cast rare-earth-free magnesium alloy with secondary particles. Thus, the present study eventually helps in identifying the rate controlling mechanism at low stresses (<50 MPa) while validating the efficacy of the newly built horizontal creep frame.

Accordingly, the objectives of this present study include (a) the design and construction of a versatile creep machine for creep testing without pre-load, (b) the design of a machine capable of creep testing over a wide range of load (from as low as 5 N) and temperature with provision for attachment such as DIC, and (c) testing the applicability of the in-house-built creep testing machine on miniaturized Mg-alloy specimens over a wide stress range of 1.6–80 MPa (corresponding load range of 6.4–310 N).

II. DESIGN AND CONSTRUCTION OF THE HORIZONTAL CREEP TESTING MACHINE

The horizontal creep testing machine developed in this study is an improved model of a typical constant dead load vertical loading creep testing machine. The plan views of this machine are shown in Fig. 1. Figures 1(a)–1(c) represent

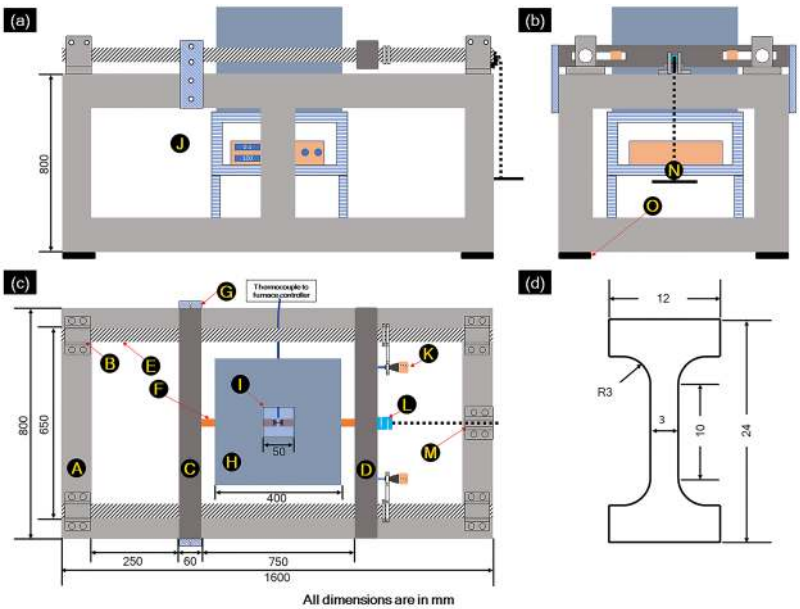

A - Base frame, B - End support blocks, C - Upper cross head, D - Lower cross head, E - Support shaft, F - Pull rods, G - Cross head clamps, H - Furnace, I - Quartz window, J - Furnace controller, K - Digimatic indicator, L - S-type load cell, M - Sprocket housing, N - Load pan, O - Anti vibration pads

FIG. 1. Plan views of the in-house-built horizontal type creep testing machine: (a) front plan view, (b) side plan view, (c) top plan view (important parts are indicated in capital letters), and (d) schematic drawing of tensile specimen used for creep testing.

TABLE II. List of the essential components and their specifications together with supplier details.

Part index	Part name	Specification/make
A	Base frame	Commercially available AISI 1018 C-channels with dimensions $150 \times 75 \times 9$ mm^3
B	End support blocks	THK India Pvt. Ltd, India
C	Upper crosshead	Commercially available EN-8 steel
D	Lower crosshead	Commercially available EN-8 steel
E	Support shaft	40 mm diameter, THK India Pvt. Ltd, India
F	Pull rods	IN718 superalloy rod of 18 mm diameter
G	Crosshead clamps	Commercially available EN-8 steel
H	Furnace	A1-Kanthal heating element, resistance type furnace/Indfurr Superheat Furnaces, Chennai, India
I	Quartz window	Commercially available
J	Furnace controller	Indfurr Superheat Furnaces, Chennai, India
K	Digimatic indicator	Total displacement 30 mm travel, 0.5 μm resolution/Mitutoyo digimatic indicator (Mitutoyo Ltd., Japan) attached to T-Box data logger/Bobe Instruments, Sylbacher Straße, Lage/Lippe, Germany
L	S-type load cell	5 kN capacity/Spanktronics Pvt. Ltd, Bengaluru, India
M	Sprocket housing	Martin Sprockets (Arlington, Texas, USA)
N	Load pan	Commercially available EN-8 steel
O	Anti-vibration pads	Commercially available

the front view, side view, and top view, respectively, and the parts are referred with capital letters (refer Table II for complete details of the parts). The dimensions of the actual parts are specified in the plan views, and some of the parts are drawn to the dimensional ratio for readability. All the important components in this horizontal creep testing frame, their manufacturer, and primary specifications are listed in Table II. The complete details of the parts (/components) are discussed in the following sub-sections.

Also, the representative dimensions and the drawing of the tensile specimen used for testing are shown in Fig. 1(d). Further, the actual in-house-built horizontal creep testing machine is shown in Fig. 2(a), and major components are indexed with letters (refer to Fig. 1 and Table II for description of components). A top view of the specimen clamps with the specimen within the box furnace is shown in Fig. 2(b). The specific details of the horizontal creep frame are described based on the following three modules:

1. Base frame—housing for the components
2. Loading system and specimen gripping fixtures
3. Strain measurement, high-temperature facility, and data acquisition

A. Base frame—Housing for the components

The principal component in the current creep testing machine is its base frame (Part-A), which dictates the rigidity and stiffness of the frame. This part also governs the maximum load that can be applied on a typical tensile/compression specimen. Commercially available mild steel (AISI 1018) C-channels with dimensions $150 \times 75 \times 9$ mm^3 were utilized to construct the base of this frame. The base frame (with all the attached parts) is mounted on anti-vibration pads (Part-O) to isolate the load train and other critical components from vibrations. The uniaxial loading of the specimen is accomplished between the two rigid crossheads made of commercially available EN-8 steel. Also, the crossheads were designed to have high stiffness (k–N/mm) that can withstand up to a load of 1000 N. To perform the tensile creep test between the two crossheads, the stationary crosshead (Part-C) is fixed to the base frame using crosshead clamps (Part-G). The mobile

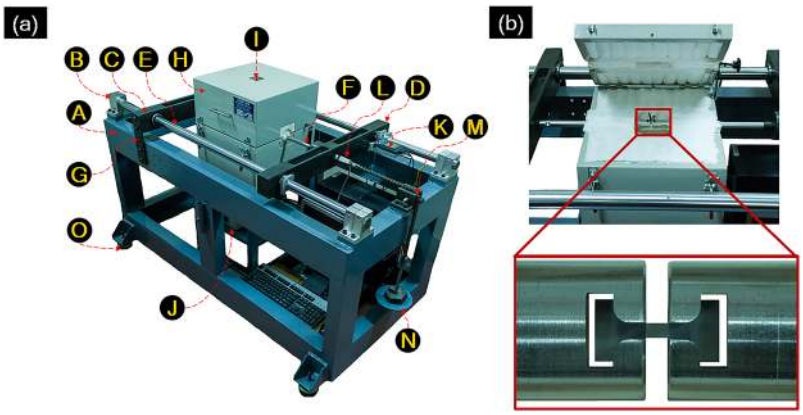

FIG. 2. In-house-built horizontal type creep testing machine at IIT Madras: (a) horizontal type constant load creep testing machine (refer to Fig. 1 and Table II for description of the parts indicated in capital letters) and (b) close-up view of the specimen and gripping region within the box furnace.

crosshead (Part-D) is allowed to slide linearly and parallel to the loading axis with negligible drag force (<2.5 N), whose linear movement is accomplished using a combination of a low friction linear bush (made by THK India Pvt. Ltd, India) and linear shaft (Part-E). The linear shafts (Part-E) deployed here are made of a corrosion resistant stainless-steel shaft of diameter 40 mm (THK India Pvt. Ltd, India). These two shafts are rigidly fixed to the upper portion of the base frame using the end support blocks (Part-B) made of aluminum.

B. Loading system and specimen gripping fixtures

To conduct the creep testing at high temperatures, pull rods together with specimen gripping fixtures that are oxidation resistant, creep resistant, and of high strength are essential. To achieve this, Ni-base superalloy (IN718) rods with the M16 thread at both ends are used as pull rods (Part-F). Further, clamps made of Ni-base superalloys (IN718) are used to hold the specimen, which are fixed to pull rods. The usage of the high-performance superalloy as pull rods and clamp material ensures that even at higher temperatures, the stiffness of the load train assembly is not compromised. Besides, these IN718 superalloy pull rods and clamps ensure that conducting creep testing up to a temperature of 700 °C and at loads up to 1000 N is accomplished. In addition, one can also use MAR-M246/MAR-M247 superalloys if the creep machine is intended to be used for the testing beyond 700 °C. The detailed top view of the specimen clamps used in the present study for tensile type loading (dog-bone shaped tensile specimen) is shown in Fig. 2(b). Although the specimen clamps shown here are specifically used for tensile loading, it is pertinent to mention that appropriate compression specimen holders and inserts can also be accommodated for compression creep testing in the current creep frame. To measure the load applied on the specimen, an S-type load cell (Spanktronics Pvt. Ltd., Bengaluru, India) (Part-I) with a maximum load capacity of 5 kN is installed in the present setup. The load cell is connected between the movable crosshead (Part-D) and the load pan (Part-N). It is important to mention that for creep testing at a low load range of <50 N, it is advised to connect the load cell between the stationary crosshead (Part-C) and the stationary pullrod (Part-F). Such a measure will eliminate the redundant forces viz. plunge force (maximum of 2.5 N) to move the stylus of the digimatic indicator and friction forces from the bearings (maximum of 2.5 N) and thus indicates the actual force on the specimen accurately.

The load-pan (Part-N) which houses the dead weight is connected to the S-type load cell using an industry standard bush roller chain and sprocket (Part-M). The chain and sprocket used in the present creep testing machine are procured from Martin Sprockets (Arlington, Texas, USA). The friction force in chain sprocket and load assembly is an important parameter that dictates the sensitivity of the machine at loads <20 N. The presence of unwanted friction forces result in an anomaly while recording the strain such as an abrupt change or negligible change in strain at strain rates lower than 10^{-8} s^{-1}. The absence of sharp strain changes (viz. strain dwell over a period of time, followed by a sudden increase in the strain) even at low loads of <20 N and large elongation reveals the stability and accuracy of the horizontal creep testing machine. Extra care is taken to ensure that the loading axis and the specimen axis were aligned using the spirit level and dial test indicators along the loading axis.

C. Strain measurement, high-temperature facility, and data acquisition

To obtain a reliable and repeatable creep testing data at elevated temperatures, a high-temperature furnace together with a reliable temperature controller is essential. The present creep testing machine is equipped with a split type resistance heating electric furnace (Indfurr Superheat Furnaces, Chennai, India) (Part-H) with A1-type Kanthal heating element. The temperature controller can control the temperature to an accuracy of 0.5 K, which enhances the reliability of the creep machine. A uniform temperature zone of $75 \times 75 \times 75$ mm^3 has been attained. A K-type thermocouple is placed (~2 mm away from the specimen surface) above the middle of the specimen. A temperature gradient of ±2 K is observed along the length and width direction across the uniform temperature zone in various creep tests conducted in the temperature range of 175–450 °C.

Measurement of displacement as a function of time is the primary requirement during the creep testing. As the sample undergoes plastic deformation during creep testing, it results in the displacement of the movable crosshead. The digimatic indicator (Part-K) (Mitutoyo Ltd., Japan) with a total travel span of 30 mm is used to measure the displacement of the movable crosshead. The resolution of the digimatic indicator is 0.5 μm, and considering a gauge length of 10 mm, the minimum strain that can be measured using this unit is as low as 0.005%. The displacement is recorded at a predefined interval using T-Box data logger (Bobe Instruments, Sylbacher Straße, Lage/Lippe, Germany). Besides the strain measurement via the digimatic indicator, another provision has been made for an independent strain measurement using the more advanced techniques such as digital image correlation (DIC). To accommodate the DIC setup, a quartz window of $50 \times 50 \times 2$ mm^3 is accommodated on the top closure of the split furnace, which is positioned over the specimen region. In the present study, the DIC setup is not used, and the strains presented in the current report are from the digimatic indicator only. However, the strain measurement using DIC during creep testing was carried out in another horizontal creep machine (HCM2), and the discussion on the similar machine is presented in detail in the supplementary material.

III. EFFICACY OF THE IN-HOUSE-BUILT HORIZONTAL CREEP TESTING MACHINE BY CREEP TESTING OF Mg-BASE TX11 (Mg-1 wt. % Sn-1 wt. % Ca) ALLOY

The objective of this section is three-fold: (a) validating the lower load range (as low as 6.4, 9.3, 11.3, 15, and 18.1 N) capability of the creep testing machine by conducting creep tests of the TX11 alloy, (b) wide temperature range (175–450 °C) and load range (6.4–310 N; corresponding to the initial stress range of 1.6–80 MPa) testing competence of this machine by conducting constant tensile load creep testing on the same Mg-base TX11 alloy (Mg-1 wt. % Sn-1 wt. % Ca),

and (c) tensile creep characterization of the same Mg-base alloy in the above temperature and stress range.

The alloy chosen for the present creep study is a permanent mold cast TX11 alloy (Mg–1 wt. % Sn–1 wt. % Ca). Since the primary objective of this work is to validate the horizontal creep testing frame specifically for very low load testing, the detailed casting procedure and characterization of the Mg-base alloy are not discussed here. To characterize and identify the phases present in the as-cast condition, scanning electron microscopy (SEM) was carried out using INSPECT-F at 20 kV and the corresponding microstructure imaged in the backscattered electron (BSE) mode is shown in Fig. 3. The alloy TX11 primarily consists of α-Mg (solid solution of Mg–Ca–Sn), CaMgSn (particles), and a minor fraction of eutectic phase (α-Mg + Mg_2Ca). Constant load tensile creep tests were performed using dog bone shaped [Fig. 1(d)] samples in the load range of 6.4–18 N (corresponding to an applied initial stress range of 1.6–5.9 MPa) and at a constant temperature of 450 °C. Similarly, few more creep experiments were also conducted at a lower temperature of 175 °C and in the load range of 70–300 N (corresponding to an initial applied stress range of 20–80 MPa). Before the application of load, the specimen was aligned and clamped precisely using the alignment fixtures. No preload was applied on the specimen before application of the actual load. An hour after reaching the test temperature, the total dead load corresponding to the chosen stress was applied. The temperature was maintained within ±2 °C throughout the creep test. The temperature during testing was monitored using a K-type thermocouple placed near the specimen. The displacement was acquired at a frequency of 1 Hz using a digimatic indicator, immediately after the application of load. In the present study, the strain reported is the strain accrued during the creep deformation only, and the instantaneous strain is not considered. The creep experiments at a test temperature of 175 °C and at an applied stress ≤60 MPa were stopped after a duration of 200 h, whereas creep tests at an applied stress >60 MPa were continued till failure. Similarly, creep tests at 450 °C were terminated after reaching the minimum strain rate.

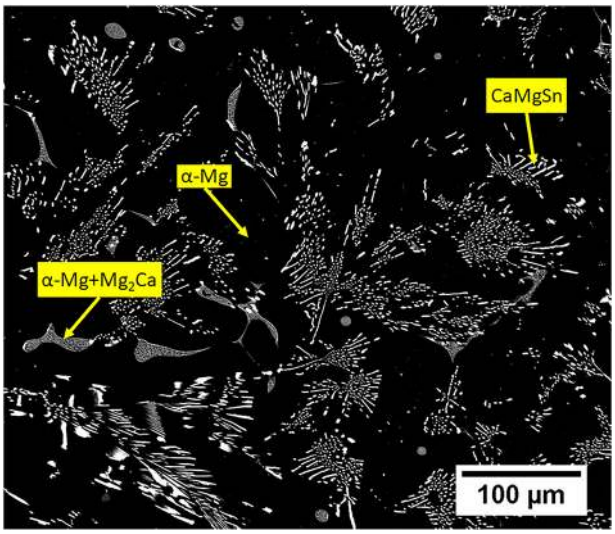

FIG. 3. Backscattered scanning electron micrograph of TX11 (Mg–1 wt. % Sn–1 wt. % Ca) magnesium alloy showing various phases: fine bright regions are CaMgSn particles, the dark region is α-Mg (solid solution of Mg–Ca–Sn), and the gray phase is the eutectic phase (α-Mg + Mg_2Ca).

The representative creep curves at respective test temperatures are shown in Figs. 4(a)–4(c). The creep curves at 175 °C and at an applied stress range of 20–80 MPa are shown in Fig. 4(a). Since the creep strain (ε) is less than 4% for stresses <60 MPa even after 200 h and is not resolved clearly in Fig. 4(a), the curves are replotted up to a strain (ε) of 2% and are shown in Fig. 4(b). Similarly creep curves at a test temperature of 450 °C are shown in Fig. 4(c). It is important to mention that the minimum applied test load at 450 °C is 6.4 N, and the corresponding creep curve [Fig. 4(c), green curve] shows the resolution merit of the current horizontal type creep testing machine. Creep tests at 3.6 and 5.1 MPa stress were repeated [represented with open legends in Figs. 4(c) and 5(b)], and the data clearly suggest that the present testing method and the horizontal creep machine are capable of producing the reproducible results in remarkable fashion. Similarly, the creep curve at the higher applied load is 11.3 N (just 2 N higher than 9.3 N), and it is worthwhile to note that such a small change in load (corresponding stress change of ~1.0 MPa) has resulted in a remarkable resolvable difference in the creep curve for the TX11 magnesium alloy. In addition, macroscopic images of the specimens after creep testing are shown in Fig. 4(d). This macrograph clearly illustrates that the deformation is uniform within the gauge length and confined to the gauge length. Thus, in a commendable fashion, it was verified that the creep testing in the abysmally small load range and at a higher temperature is possible with the in-house-built horizontal creep testing machine.

Figure 5(a) illustrates the creep rate ($\dot{\varepsilon}$) as a function of creep strain (ε) at a constant temperature of 175 °C, and the closer view of these curves up to a strain of 1% is shown in the inset of Fig. 5(a). A closer look at the inset in Fig. 5(a) shows that the curve at 60 MPa falls slightly below 50 MPa up to a strain of ~0.4%. However, the steady state strain rate (which is considered for further analysis) corresponding to 60 MPa is clearly above that of 40 and 50 MPa curves [corresponding creep strain-time curve in Fig. 4(b) is also consistent with this observation]. This could be attributed for not considering the instantaneous strain (i.e., the strain accrued immediately after the application of the actual load) prior to the start of the actual creep test. It has resulted in the appearance of the 60 MPa curve at lower strain rates (although it should have started toward the right as well as above that of the 50 MPa curve) as compared to 50 MPa. However, this visual discrepancy between the 60 MPa and 50 MPa curves does not affect the further analysis while evaluating the creep parameters and consequent analysis of deformation mechanism.

In the stress range of 45–60 MPa, initially, the creep rate decreases up to a strain of ~1% followed by an increase in the creep rate up to ~2% and then the creep rate decreases with further deformation which indicates that the material is undergoing strain hardening. At an applied stress of 70 and 80 MPa, the tertiary state is observed after ~10% strain, whereas at stress <45 MPa, the creep rate decreases continuously. The observed strain rates during the testing are in the range of 10^{-5}–10^{-10} s^{-1}. At the test temperature of 450 °C,

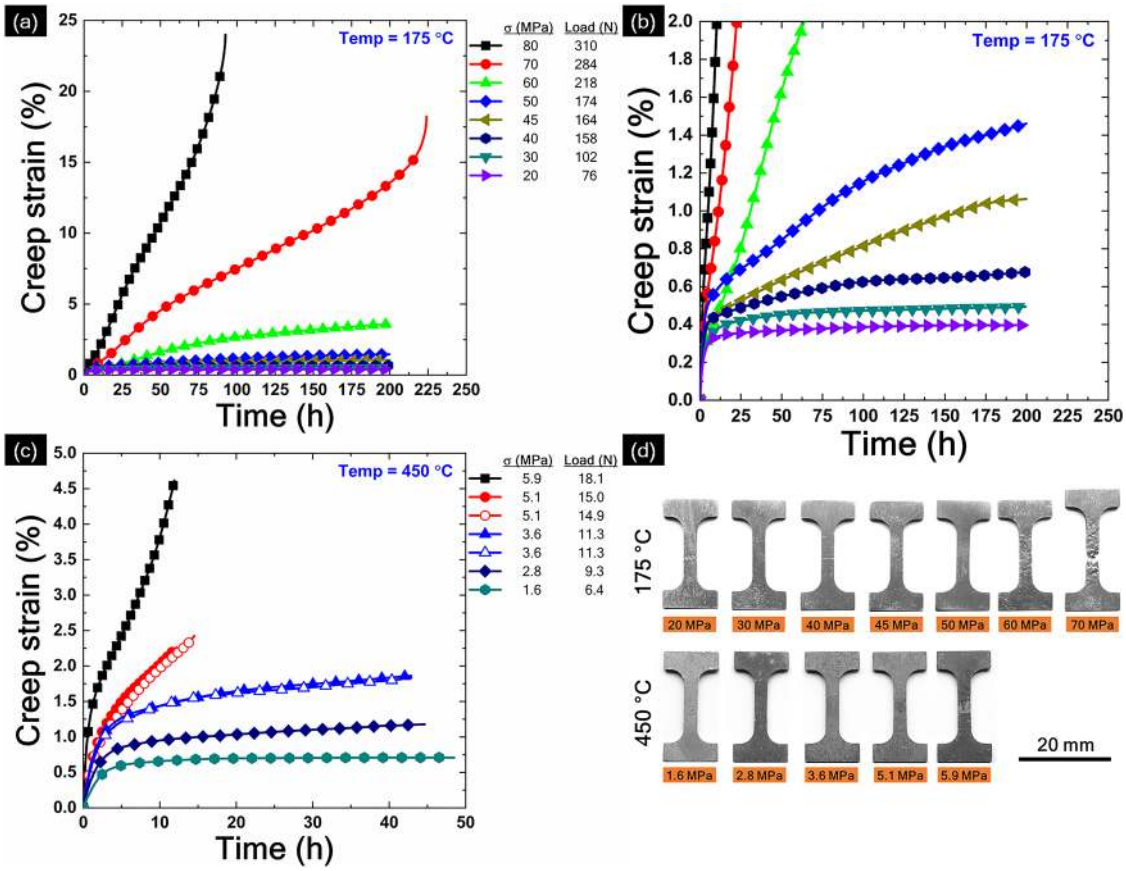

FIG. 4. Typical creep curves in the form of variation of creep strain with time for the TX11 alloy tested (a) up to fracture in the stress range of 20–80 MPa (equivalent load range of 76–310 N) and at a constant temperature of 175 °C, (b) up to a strain of 2% (under the same testing conditions) shown for the sake of better clarity, (c) at lower stress range of 1.6–5.9 MPa (equivalent load range of 6.4–18.1 N) at a constant temperature of 450 °C; open symbols (blue and red) represent tests at 3.6 and 5.1 MPa illustrating the repeatability of creep data; (d) macroscopic image of samples after creep testing at 175 °C and 450 °C (applied stress during testing is specified below the specimen).

the strain rate decreases and reaches a minimum strain rate and the respective creep curves are shown in Fig. 5(b). It is important to note that the measurement of such low strain rates at a very low temperature of 175 °C and at low loads (<10 N) at 450 °C illustrates the reliability and efficacy of the in-house-built horizontal creep testing machine.

Figure 6 represents the minimum strain rate as a function of applied stress on a double logarithmic scale. The slope of the curve represents the stress exponent (n) according to the following equation:

$$\dot{\varepsilon} = B\sigma^n, \tag{1}$$

where $\dot{\varepsilon}$ – strain rate (s^{-1}), B – constant, σ – applied stress (MPa), and n – stress exponent.

Since the strain rate vs. creep strain curves at 175 °C exhibit multiple minimum creep rates for applied stress >45 MPa, the minimum creep rate observed for the strain less than 2% is considered for the present analysis. Whereas, at 450 °C, the minimum strain rate is observed only once and is considered for evaluating the stress exponent. It is evident from Fig. 6 that at 175 °C, there is a transition in the stress exponent (n) with applied stress (n ~ 6.8 at >50 MPa and n ~ 10 at 40-50 MPa). Similarly, the strain rate observed at 450 °C was $>10^{-9}$ s^{-1} and the stress exponent (n ~ 4.8) is constant over the tested stress range. A stress exponent of 4.8 indicates that dislocation climb could be the rate controlling mechanism. Variation of the stress exponent at 175 °C can be primarily attributed to the CaMgSn particle in the α-Mg solid solution. Interaction of dislocations with solute atoms and with second phase could result in a change in the rate controlling (viscous glide/climb) mechanism with applied stress.[38] This could be a possible reason for the variation of the stress exponent at 175 °C. The detailed discussion on the deformation mechanism of the present Mg-alloy is beyond the scope of the present article, and those detailed creep studies on this alloy will be communicated elsewhere as an independent manuscript.

It is important to mention that besides the present horizontal creep testing machine (HCM1), a similar horizontal creep testing machine (HCM2) was established by one of the co-authors (RK) in another laboratory at the Department of Materials Engineering, Indian Institute of Science, Bengaluru, India. Further, on HCM2, the high temperature creep experiments were successfully conducted on pure aluminum both in tension and in compression. More importantly, the strain measurements during creep deformation were successfully captured using the digital image correlation (DIC) technique on HCM2. The details of the creep experiments, strain measurements by DIC, and results from HCM2 are presented in the supplementary material.

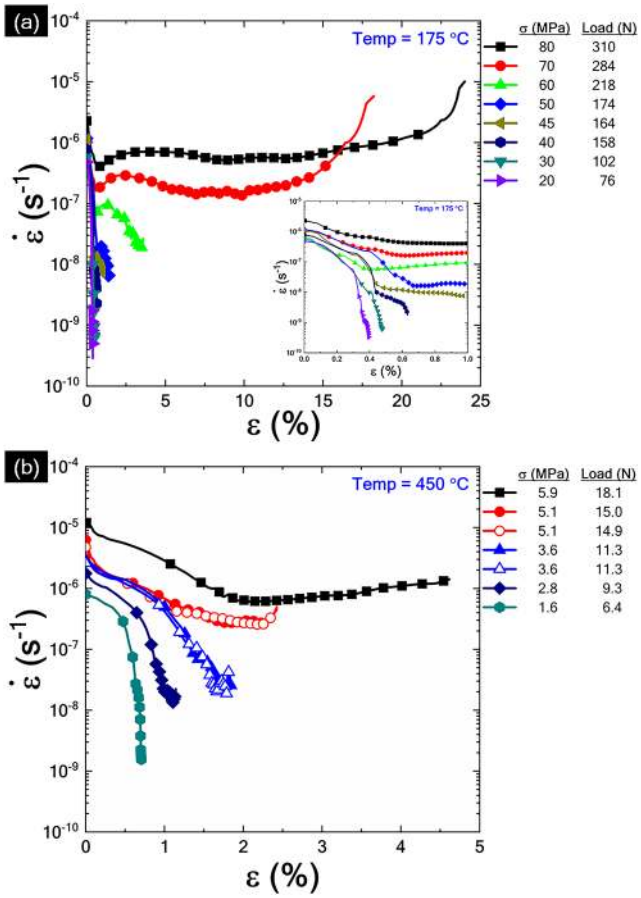

FIG. 5. Variation of strain rate ($\dot{\varepsilon}$) with creep strain (ε) for alloy TX11 tested at different stress levels (a) at 175 °C; the inset shows the enlarged view of strain rate variation with creep strain at strain <0.01 and (b) at 450 °C. Excellent repeatability is illustrated by the red (open and filled circle legends) and blue (open and filled triangle legends) lines that represent the repeated tests at 5.1 and 3.6 MPa, respectively.

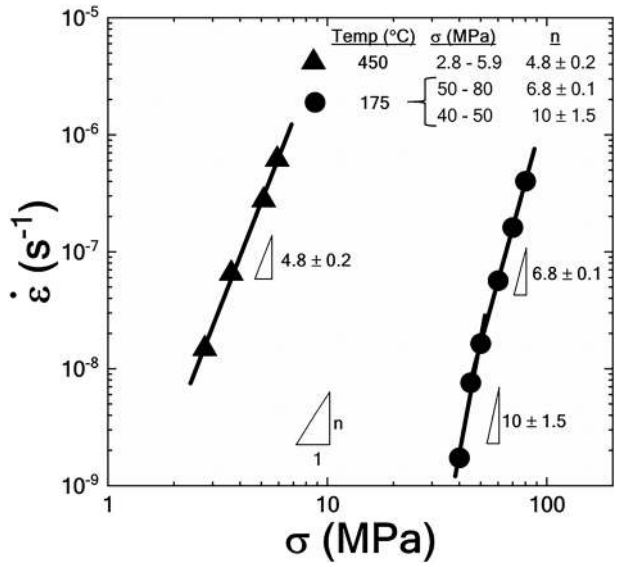

FIG. 6. Double logarithmic plot showing the strain rate ($\dot{\varepsilon}$) dependence of applied stress (σ) at temperatures 175 °C (filled circles) and 450 °C (filled triangles) illustrating the evaluation of the stress exponent (n).

IV. SUMMARY AND CONCLUSIONS

In the present study, design, fabrication, and validated testing of the in-house-built horizontal creep testing machine is successfully presented. The following are the major conclusions.

a. It has been demonstrated with utmost confidence that the in-house-built horizontal creep frame can be utilized to conduct creep testing with a negligible preload on low melting point alloys such as Mg-alloys at very low loads of ~6 N. Thus, this versatile machine can be utilized to understand the high temperature creep behavior of Mg-base alloys and Al-base alloys even in the very low stress range as well as on the miniaturized specimens.
b. Tensile creep characterization of Mg-base alloy TX11 over a wide range of loads ranging from ~6 to 300 N (corresponding stress range of 1.6–80 MPa) and at a lower temperature of 175 °C as well as at 450 °C was demonstrated successfully.
c. Further, this machine can find its versatility to conduct creep testing of additively manufactured components (any material) of various small-scale dimensions and creep testing of weldments with minimal modifications of the fixtures depending on the testing method and attachments (compression and DIC/video extensometer) to characterize the local creep behavior of materials with complex and heterogeneous microstructures.

SUPPLEMENTARY MATERIAL

In supplementary material, the design of another horizontal creep machine (HCM2) similar to HCM1 (creep machine presented in the main text) is illustrated. The additional capabilities of performing high temperature creep experiments under both tension and compression using a Digital Image Correlation (DIC) attachment to measure local strain on the aluminum specimen are demonstrated.

ACKNOWLEDGMENTS

Rajesh Korla (IIT Hyderabad) and Ravi Sankar Kottada (IIT Madras) are extremely grateful to their Ph.D. adviser Professor Atul H. Chokshi of Department of Materials Engineering, Indian Institute of Science, Bengaluru, India, for providing ample freedom and also for sharing his wisdom and insights while building these creep machines. We sincerely thank two anonymous reviewers for their critical review and constructive comments on our first version of the manuscript. Their comments have certainly helped us bring more scientific rigorousness and clarity in our article.

[1]M. E. Kassner, *Fundamentals of Creep in Metals and Alloys* (Butterworth-Heinemann, 2015).
[2]J.-P. Poirier, *Creep of Crystals: High-Temperature Deformation Processes in Metals, Ceramics, and Minerals* (Cambridge University Press, 1985).
[3]B. Mordike and T. Ebert, Mater. Sci. Eng.: A **302**, 37 (2001).
[4]A. V. Nagasekhar, C. H. Cáceres, and C. Kong, Mater. Charact. **61**, 1035 (2010).
[5]A. A. Luo, Int. Mater. Rev. **49**, 13 (2004).
[6]N. D. Saddock, A. Suzuki, J. W. Jones, and T. M. Pollock, Scr. Mater. **63**, 692 (2010).

[7]T. Trosch, J. Strößner, R. Völkl, and U. Glatzel, Mater. Lett. **164**, 428 (2016).
[8]M. N. Gussev, J. T. Busby, K. G. Field, M. A. Sokolov, and S. E. Gray, *Small Specimen Test Techniques* (ASTM International, 2014), Vol. 6.
[9]T. H. Hyde, W. Sun, and J. A. Williams, Int. Mater. Rev. **52**, 213 (2007).
[10]E. N. da C. Andrade, Proc. R. Soc. A **84**, 1 (1910).
[11]E. N. da C. Andrade and B. Chalmers, Proc. R. Soc. A **138**, 348 (1932).
[12]A. Nadai and J. Boyd, U.S. patent 2,154,280 (11 April 1939).
[13]L. M. T. Hopkin, Proc. Phys. Soc. Sect. B **63**, 346 (1950).
[14]A. J. Kennedy and R. F. Slade, J. Sci. Instrum. **33**, 409 (1956).
[15]R. C. Boettner and W. D. Robertson, Rev. Sci. Instrum. **27**, 1039 (1956).
[16]T. D. Dudderar, Rev. Sci. Instrum. **40**, 1231 (1969).
[17]A. A. Solomon, Rev. Sci. Instrum. **40**, 1025 (1969).
[18]W. A. Coghlan, Rev. Sci. Instrum. **43**, 464 (1972).
[19]P. Yavari and T. Langdon, J. Test. Eval. **10**, 174 (1982).
[20]R. B. Grishaber, R. H. Lu, D. M. Farkas, and A. K. Mukherjee, Rev. Sci. Instrum. **68**, 2812 (1997).
[21]M. Kolbe, J. Murken, D. Pistolek, G. Eggeler, and H.-J. Klam, Materialwiss. Werkstofftech. **30**, 465 (1999).
[22]R. Völkl and B. Fischer, Exp. Mech. **44**, 121 (2004).
[23]L. Luan, H. Riesch-Oppermann, and M. Heilmaier, J. Mater. Res. **32**, 4563 (2017).
[24]ASTM E139-11, *Standard Test Methods for Conducting Creep, Creep-Rupture, and Stress-Rupture Tests of Metallic Materials* (ASTM International, 2011).
[25]X. Wu, P. Wollgramm, C. Somsen, A. Dlouhy, A. Kostka, and G. Eggeler, Acta Mater. **112**, 242 (2016).
[26]D. Kurumlu, E. J. Payton, M. L. Young, M. Schöbel, G. Requena, and G. Eggeler, Acta Mater. **60**, 67 (2012).
[27]M. C. Askins and K. D. Marchant, *Remaining-Life Estimation of Boiler Pressure Parts: Volume 2, Miniature Specimen Creep Testing* (Central Electricity Research Laboratory, Leatherhead, UK, 1988).
[28]K. Sonoya, M. Kitagawa, M. Murata, H. Tanaka, and K. Yagi, J. Soc. Mater. Sci., Jpn. **43**, 348 (1994).
[29]N. F. Panayotou, R. J. Puigh, and E. K. Opperman, J. Nucl. Mater. **104**, 1523 (1981).
[30]A. Garzillo, C. Guardamagna, L. Moscotti, and L. Ranzani, Int. J. Pressure Vessels Piping **66**, 223 (1996).
[31]G. Mälzer, R. W. Hayes, T. Mack, and G. Eggeler, Metall. Mater. Trans. A **38**, 314 (2007).
[32]A. Takada, M. Sakane, and Y. Tsukada, in *ASME 2005 International Mechanical Engineering Congress and Exposition* (American Society of Mechanical Engineers, 2005), p. 265.
[33]B. Skrotzki, K. Neuking, C. Mayr, and G. Eggeler, Materialwiss. Werkstofftech. **29**, 137 (1998).
[34]J. Olbricht, M. Bismarck, and B. Skrotzki, Mater. Sci. Eng.: A **585**, 335 (2013).
[35]A. C. Lewis, D. van Heerden, C. Eberl, K. J. Hemker, and T. P. Weihs, Acta Mater. **56**, 3044 (2008).
[36]R. Völkl, B. Fischer, M. Beschliesser, and U. Glatzel, Mater. Sci. Eng.: A **483**, 587 (2008).
[37]H. Kanayama, N. Hiyoshi, T. Itoh, F. Ogawa, and T. Wakai, J. Soc. Mater. Sci., Jpn. **66**, 86 (2017).
[38]B. Han and D. Dunand, Mater. Sci. Eng.: A **300**, 235 (2001).
[39]P. Shahbeigi Roodposhti, A. Sarkar, K. L. Murty, and R. O. Scattergood, J. Mater. Eng. Perform. **25**, 3697 (2016).
[40]S. S. Vagarali and T. G. Langdon, Acta Metall. **30**, 1157 (1982).
[41]A. A. Luo, B. R. Powell, and M. P. Balogh, Metall. Mater. Trans. A **33**, 567 (2002).